

Published in final edited form as:

*Nature*. 2011 January 13; 469(7329): 241–244. doi:10.1038/nature09746.

## The structural basis for agonist and partial agonist action on a $\beta_1$ -adrenergic receptor

Tony Warne, Rouslan Moukhametzianov, Jillian G. Baker<sup>1</sup>, Rony Nehmé, Patricia C. Edwards, Andrew G.W. Leslie, Gebhard F.X. Schertler<sup>2,\*</sup>, and Christopher G. Tate<sup>\*</sup>  
MRC Laboratory of Molecular Biology, Hills Road, Cambridge CB2 0QH, UK

<sup>1</sup>Institute of Cell Signalling, C Floor Medical School, Queen's Medical Centre, University of Nottingham, Nottingham NG7 2UH, UK

$\beta$ -Adrenergic receptors ( $\beta$ ARs) are G protein-coupled receptors (GPCRs) that activate intracellular G proteins upon binding catecholamine agonist ligands such as adrenaline and noradrenaline<sup>1,2</sup>. Synthetic ligands have been developed that either activate or inhibit  $\beta$ ARs for the treatment of asthma, hypertension or cardiac dysfunction. These ligands are classified as either full agonists, partial agonists or antagonists, depending on whether the cellular response is similar to that of the native ligand, reduced or inhibited, respectively. However, the structural basis for these different ligand efficacies is unknown. Here we present four crystal structures of the thermostabilised turkey (*Meleagris gallopavo*)  $\beta_1$ -adrenergic receptor ( $\beta_1$ AR-m23) bound to the full agonists carmoterol and isoprenaline and the partial agonists salbutamol and dobutamine. In each case, agonist binding induces a 1 Å contraction of the catecholamine binding pocket relative to the antagonist bound receptor. Full agonists can form hydrogen bonds with two conserved serine residues in transmembrane helix 5 (Ser<sup>5.42</sup> and Ser<sup>5.46</sup>), but partial agonists only interact with Ser<sup>5.42</sup> (superscripts refer to Ballesteros-Weinstein numbering<sup>3</sup>). The structures provide an understanding of the pharmacological differences between different ligand classes, illuminating how GPCRs function and providing a solid foundation for the structure-based design of novel ligands with predictable efficacies.

Determining how agonists and antagonists bind to the  $\beta$  receptors has been the goal of research for more than 20 years<sup>4-11</sup>. Although the structures of the homologous  $\beta_1$  and  $\beta_2$  receptors<sup>12-15</sup> show how some antagonists bind to receptors in the inactive state<sup>16</sup>, structures with agonists bound are required to understand subsequent structural transitions involved in activation. GPCRs exist in an equilibrium between an inactive state (R) and an activated state (R\*) that can couple and activate G proteins<sup>17</sup>. The binding of a full agonist, such as adrenaline or noradrenaline, is thought to increase the probability of the receptor converting to R\*, with a conformation similar to that of opsin<sup>18,19</sup>. In the absence of any ligand, the  $\beta$ ARs exhibit a low level of constitutive activity, indicating that there is always a small

\*Joint corresponding authors: MRC Laboratory of Molecular Biology, Hills Road, Cambridge CB2 0QH, UK, cgt@mrc-lmb.cam.ac.uk, gebhard.schertler@psi.ch, Telephone +44-(0)1223-402266, Fax +44-(0)1223-213556.

<sup>2</sup>Current Address: Paul Scherrer Institut, Laboratory of Biomolecular Research, BMR, OFLC 109, CH-5232 Villigen PSI, Switzerland, Telephone +41 (0)56 310 4265

**Author contributions:** T.W. devised and performed receptor expression, purification, crystallization, cryo-cooling of the crystals, data collection and initial data processing. P.C.E. helped with crystal cryo-cooling and data collection. J.G.B. performed the pharmacological analyses on receptor mutants in whole cells and R.N. performed the ligand binding studies on baculovirus-expressed receptors. R.M. and A.G.W.L. were involved in data processing and structure refinement. Manuscript preparation was performed by T.W., C.G.T., A.G.W.L. and G.F.X.S. The overall project management was by G.F.X.S. and C.G.T.

**Author Information:** Co-ordinates and structure factors have been submitted to the PDB database under accession codes 2y00, 2y01, 2y02, 2y03 and 2y04 for  $\beta_1$ -m23 bound either to dobutamine (dob92 and dob102), carmoterol, isoprenaline or salbutamol, respectively.

proportion of the receptor in the activated state, with the  $\beta_2$ AR showing a 5-fold higher level of basal activity than the  $\beta_1$ AR<sup>20</sup>. Basal activity of  $\beta_2$ AR is important physiologically, as shown by the T164I<sup>4,56</sup> human polymorphism that reduces the basal activity of  $\beta_2$ AR to levels similar to  $\beta_1$ AR<sup>21</sup> and whose expression has been associated with heart disease<sup>22</sup>.

As a first step towards understanding how agonists activate receptors, we have determined the structures of  $\beta_1$ AR bound to 4 different agonists. Native turkey  $\beta_1$ AR is unstable in detergent<sup>23</sup>, so crystallization and structure determination relied on using a thermostabilised construct ( $\beta_1$ AR-m23) that contained six point mutations, which dramatically improved its thermostability<sup>24</sup>. In addition, the thermostabilising mutations altered the equilibrium between R and R\*, so that the receptor was preferentially in the R state<sup>24</sup>. However, it could still couple to G proteins after activation by agonists<sup>13</sup> (Supplementary Fig. 1, Supplementary Tables 1-3), although the activation energy barrier is predicted to be considerably higher than for the wild-type receptor<sup>25</sup>. Here we report structures of  $\beta_1$ AR-m23 (see Methods) bound to *r*-isoprenaline (2.85 Å resolution), *r,r*-carmoterol (2.6 Å resolution), *r*-salbutamol (3.05 Å resolution) and *r*-dobutamine (two independent structures at 2.6 Å and 2.5 Å resolution) (Supplementary Table 5). The overall structures of  $\beta_1$ AR-m23 bound to the agonists are very similar to the structure with the bound antagonist cyanopindolol<sup>13</sup>, as expected for a receptor mutant stabilised preferentially in the R state. None of the structures show the outward movement of the cytoplasmic end of transmembrane helix H6 by 5-6 Å that is observed during light activation of rhodopsin<sup>18, 19, 26</sup>. This suggests that the structures represent an inactive, non-signaling state of the receptor formed on initial agonist binding.

All four agonists bind in the catecholamine pocket in a virtually identical fashion (Fig. 1). The secondary amine and  $\beta$ -hydroxyl groups shared by all the agonists (except for dobutamine, which lacks the  $\beta$ -hydroxyl; see Supplementary Figure 4) form potential hydrogen bonds with Asp121<sup>3,32</sup> and Asn329<sup>7,39</sup>, while the hydrogen bond donor/acceptor group equivalent to the catecholamine *meta*-hydroxyl (*m*-OH) generally forms a hydrogen bond with Asn310<sup>6,55</sup>. In addition, all the agonists can form a hydrogen bond with Ser211<sup>5,42</sup>, as seen for cyanopindolol<sup>13</sup>, and they also induce the rotamer conformation change of Ser212<sup>5,43</sup> so that it makes a hydrogen bond with Asn310<sup>6,55</sup>. The major difference between the binding of full agonists compared to the partial agonists is that only full agonists make a hydrogen bond to the side chain of Ser215<sup>5,46</sup> as a result of a change in side chain rotamer. All of these amino acid residues involved in the binding of the catecholamine headgroups to  $\beta_1$ AR are fully conserved in both  $\beta_1$  and  $\beta_2$  receptors (Fig. 2). Furthermore, the role of many of these amino acid residues in ligand binding is supported by extensive mutagenesis studies on  $\beta_2$ AR that were performed before the first  $\beta_2$ AR structure was determined<sup>27</sup>. Thus it was predicted that Asp113<sup>3,32</sup>, Ser203<sup>5,42</sup>, Ser207<sup>5,46</sup>, Asn293<sup>6,55</sup> and Asn312<sup>7,39</sup> in  $\beta_2$ AR were all involved in agonist binding<sup>4,5,7-9</sup> (Fig. 3). Inspection of the region outside the catecholamine binding pocket in the structures with bound dobutamine and carmoterol allows the identification of non-conserved residues that interact with these ligands (Fig. 2 and Supplementary Figure 7), which may contribute to the subtype specificity of these ligands<sup>10,28</sup>.

There are three significant differences in the  $\beta_1$ AR catecholamine binding pocket when full agonists are bound compared to when an antagonist is bound, namely the rotamer conformation changes of side chains Ser212<sup>5,43</sup> and Ser215<sup>5,46</sup> (Fig.3) and the contraction of the catecholamine binding pocket by  $\sim 1$  Å, as measured between the C $\alpha$  atoms of Asn329<sup>7,39</sup> and Ser211<sup>5,42</sup> (Fig. 4). So why should these small changes increase the probability of R\* formation? Agonist binding has not changed the conformation of transmembrane helix H5 below Ser215<sup>5,46</sup>, although significant changes in this region are predicted once the receptor has reached the fully activated state<sup>18,19</sup>. The only effect that the

agonist-induced rotamer conformation change of Ser215<sup>5,46</sup> appears to have is to break the van der Waals interaction between Val172<sup>4,56</sup> and Ser215<sup>5,46</sup>, thus reducing the number of interactions between H4 and H5. As there is only a minimal interface between transmembrane helices H4 and H5 in this region (Supplementary Table 8 and Supplementary Fig. 8), this loss of interaction may be significant in the activation process. In this regard, it is noteworthy that the naturally occurring polymorphism in  $\beta_2$ AR at the H4-H5 interface, T164I<sup>4,56</sup>, converts a polar residue to a hydrophobic residue as seen in  $\beta_1$ AR (Val172<sup>4,56</sup>), which results in both reduced basal activity and reduced agonist stimulation<sup>21</sup>. This supports the hypothesis that the extent of interaction between H4 and H5 could affect the probability of a receptor transition into the activated state.

In contrast to the apparent weakening of helix-helix interactions by the agonist-induced rotamer conformation change of Ser215<sup>5,46</sup>, the agonist-induced rotamer conformation change of Ser212<sup>5,43</sup> probably results in the strengthening of interactions between H5 and H6. Upon agonist binding, Ser212<sup>5,43</sup> forms a hydrogen bond with Asn310<sup>6,55</sup> (Fig. 3) and, in addition, hydrogen bond interactions to Ser211<sup>5,43</sup> and Asn310<sup>6,55</sup> mediated by the ligand serve to bridge H5 and H6. The combined effects of strengthening the H5-H6 interface and weakening the H4-H5 interface could facilitate the subsequent movements of H5 and H6, as observed in the activation of rhodopsin.

Stabilisation of the contracted catecholamine binding pocket is probably the most important role of bound agonists in the activation process (Fig. 4). This probably requires strong hydrogen bonding interactions between the catechol (or equivalent) moiety and both H5 and H6, and strong interactions between the secondary amine and  $\beta$ -hydroxyl groups in the agonist and the amino acid side chains in helices H3 and H7. Reduction in the strength of these interactions is likely to reduce the efficacy of a ligand<sup>29</sup>. Both salbutamol and dobutamine are partial agonists of  $\beta_1$ AR-m23 (Supplementary Table 3) and human  $\beta_1$ AR. In the case of salbutamol, there are only two predicted hydrogen bonds between the headgroup and H5/H6, compared to 3-4 potential hydrogen bonds for isoprenaline and carmoterol. Dobutamine lacks the  $\beta$ -hydroxyl group, which similarly reduces the number of potential hydrogen bonds to H3/H7 from 3-4 seen in the other agonists to only 2. We propose that this weakening of agonist interactions with H5/H6 for salbutamol and H3/H7 for dobutamine is a major contributing factor in making these ligands partial agonists rather than full agonists.

The agonist-bound structures of  $\beta_1$ AR suggest there are three major determinants that dictate the efficacy of any ligand; ligand-induced rotamer conformational changes of (i) Ser212<sup>5,43</sup> and (ii) Ser215<sup>5,46</sup> and (iii) stabilization of the contracted ligand binding pocket. The full agonists studied here achieve all three. The partial agonists studied here do not alter the conformation of Ser215<sup>5,46</sup> and may be less successful than isoprenaline or carmoterol at stabilizing the contracted catecholamine binding pocket due to reduced numbers of hydrogen bonds between the ligand and the receptor. The antagonist cyanopindolol acts as a very weak partial agonist and none of the three agonist-induced changes are observed. In contrast to partial agonists, neutral antagonists or very weak partial agonists such as cyanopindolol may also have a reduced ability to contract the binding pocket due to the greater distance between the secondary amine and the catechol moiety (or equivalent). For example, the number of atoms in the linker between the secondary amine and the headgroup of cyanopindolol is 4 whereas the agonists in this study only contain 2 (Fig. 1 and Supplementary Fig. 4). A ligand with a sufficiently bulky headgroup that binds with high-affinity and which actively prevents any spontaneous contraction of the binding pocket and/or Ser<sup>5,46</sup> rotamer change, would be predicted to act as a full inverse agonist. This is indeed what is observed in the recently determined structure<sup>15</sup> of  $\beta_2$ AR bound to the inverse agonist ICI 118,551.

The significant structural similarities amongst GPCRs suggests that similar agonist-induced conformational changes to those we have observed here may also be applicable to many other members of the GPCR superfamily, though undoubtedly there will be many subtle variations on this theme.

## METHODS SUMMARY

### Expression, purification and crystallization

The  $\beta_{44}$ -m23 construct was expressed in insect cells, purified in the detergent Hega-10 and crystallized in the presence of cholesterol hemisuccinate (CHS), following previously established protocols<sup>30</sup>. Crystals were grown by vapour diffusion, with the conditions shown in Supplementary Table 4.

### Data collection, structure solution and refinement

Diffraction data were collected from a single cryo-cooled crystal (100 K) of each complex in multiple wedges at beamline ID23-2 at ESRF, Grenoble. The structures were solved by molecular replacement using the  $\beta_1$ AR structure<sup>13</sup> (PDB code 2VT4) as a model (see Online Methods). Data collection and refinement statistics are presented in Supplementary Table 5.

## Supplementary Material

Refer to Web version on PubMed Central for supplementary material.

## Acknowledgments

This work was supported by core funding from the MRC and the BBSRC grant (BB/G003653/1). Financial support for G.F.X.S was also from a Human Frontier Science Project (HFSP) programme grant (RG/0052), a European Commission FP6 specific targeted research project (LSH-2003-1.1.0-1) and an ESRF long-term proposal. J.G.B. was funded by a Wellcome Trust Clinician Scientist Fellowship. We are grateful to P. Coli and A. Rizzi of Chiesi Farmaceutici S.P.A. (Parma, Italy) for the supply of (R,R)-carmoterol. F. Gorrec is thanked for his help with crystallisation robotics. We would also like to thank beamline staff at the European Synchrotron Radiation Facility, particularly D. Flot and A. Popov at ID23-2 and F. Marshall, M. Weir, M. Congreve and R. Henderson for helpful comments on the manuscript.

## METHODS ONLINE

### Expression, purification and crystallization

The turkey (*M. gallopavo*)  $\beta_1$ AR construct,  $\beta_{36}$ -m23, contains six thermostabilising point mutations and truncations at the N-terminus, inner loop 3 and C-terminus<sup>30</sup>. Here we used the  $\beta_{44}$ -m23 construct, which differs from the previously published  $\beta_{36}$ -m23 construct only by the presence of two previously deleted amino acid residues at the cytoplasmic end of helix 6 (H6), Thr277 and Ser278. Baculovirus expression and purification were all performed as described previously<sup>30</sup>, but with the detergent exchanged to Hega-10 (0.35%) on the alprenolol affinity column. Purified receptor was competitively eluted from the alprenolol sepharose column with 0.2 mM agonist ((R)-isoprenaline, (R,S)-salbutamol, (R,S)-dobutamine or (R,R)-carmoterol). The buffer was exchanged to 10 mM Tris-HCl, pH 7.7, 100 mM NaCl, 0.1 mM EDTA, 0.35% Hega-10 and 1.0 mM agonist during concentration to 15–20 mg ml<sup>-1</sup>. Before crystallization, CHS and Hega-10 were added to 0.45–1.8 mg ml<sup>-1</sup> and 0.5–0.65 % respectively. Crystals were grown at 4°C in 200 nl sitting drops and cryo-protected by soaking in either PEG 400 or PEG 600 for ~5 minutes (Supplementary Table 4) prior to mounting on Hampton CrystalCap HT loops and cryo-cooling in liquid nitrogen.

## Data collection, structure solution and refinement

Diffraction data were collected at the European Synchrotron Radiation Facility, Grenoble with a Mar 225 CCD detector on the microfocus beamline ID23-2 (wavelength, 0.8726 Å) using a 10 µm focused beam. The microfocus beam was essential for the location of the best diffracting parts of single crystals, as well as allowing several wedges to be collected from different positions. Images were processed with MOSFLM<sup>31</sup> and SCALA<sup>32</sup>. The isoprenaline complex was solved by molecular replacement with PHASER<sup>33</sup> using the β<sub>1</sub>AR structure (PDB code 2VT4) as a model. This structure was then used as a starting model for the structure solution of the carmoterol complex. Finally, the carmoterol complex was used as a starting model for both the dobutamine complexes and for the salbutamol complex. Refinement and rebuilding were carried out with REFMAC5<sup>34</sup> and COOT<sup>35</sup> respectively. The dob92 dobutamine crystal diffracted to a higher resolution (2.5 Å) than the dob102 crystal (2.6 Å), but the dob102 dataset was more complete and less anisotropic than dob92 and gave a lower Wilson B factor (Supplementary Table 5). Dictionary entries for the agonists were created using Jligand and PRODRG<sup>36</sup>. During refinement with REFMAC5 tight non-crystallographic restraints ( $\sigma = 0.05$  Å) were applied to the majority (172) of the residues in the two molecules in the asymmetric unit, with their selection based on improvements in  $R_{\text{free}}$  values. For the salbutamol complex, where the resolution was lower (3.05 Å), all three standard rotamers were modelled for Ser211 and Ser215 side chains, and the final choice was made based on the local stereochemistry and features in the difference maps. Hydrogen bond assignments for the ligands were determined using hbplus<sup>37</sup> but allowing a maximum hydrogen-acceptor distance of 2.7 Å and a minimum angle of 89 degrees. Superposition of the different complexes was achieved by determining an initial transformation based on the 12 C-terminal residues of helix 2 (90-101) and then using the lsq\_imp option of the program O<sup>38</sup> to find the largest number of residues that could be superposed without a significant increase in the rmsd. Cutoff values of between 0.2-0.5 Å for residues to be included in the superposition were found to produce the largest number of residues while maintaining a small rmsd (< 0.15-0.3 Å), depending on the structures being compared. This was repeated using the uppermost residues of helices 3, 6 and 7 to determine the initial transformation, and all cases converged to give the same solution, with 147 residues superposed and a final rmsd of 0.28 Å for the superposition of the carmoterol and cyanopindolol structures, and lower rmsd values for superposing different agonist structures on one another. The convergence to a common solution validates this procedure for determining the optimal transformation. Validation of the final refined models was carried out using Molprobity<sup>39</sup>. Omit densities for the ligands and the surrounding side chains are shown in Supplementary Figure 3.

The two dobutamine crystals (dob92 and dob102) differed in the crystallisation buffer and pH (Supplementary Table 4) and this resulted in slightly different unit cell parameters (Supplementary Table 5) and packing arrangements. The differences between these two structures (overall r.m.s.d 0.21 Å for monomer A, 0.21 Å for monomer B) provides a measure of the influence of crystal packing forces on the detailed conformation of the receptors. The observed differences in the ligand-binding pocket for monomer B, where there are no direct lattice contacts, emphasises the conformational flexibility of this region (Supplementary Figure 6).

## Pharmacological analysis of agonist binding to the thermostabilised β<sub>1</sub>AR mutants in whole cells

Stable CHO-K1 cell lines expressing either the wild type turkey truncated receptor (βtrunc), or the β36, or the β6-m23 or the β36-m23 receptors and a CRE-SPAP reporter were used<sup>40</sup>. See Supplementary Table 1 for a description of the constructs. Cells were grown in



Dulbecco's modified Eagle's medium nutrient mix F12 (DMEM/F12) containing 10% foetal calf serum and 2mM L-glutamine in a 37°C humidified 5% CO<sub>2</sub> : 95% air atmosphere.

To analyse the affinities of agonist binding to  $\beta_1$ AR mutants <sup>3</sup>H-CGP 12177 saturation binding and competition binding experiments were performed on whole cells (Supplementary Table 1). Cell lines were grown to confluence in white-sided tissue culture 96-well view plates. <sup>3</sup>H-CGP12177 whole cell competition binding was performed as previously described<sup>41</sup> using <sup>3</sup>H-CGP 12177 in the range of 0.82 – 1.80 nM. The K<sub>D</sub> values for <sup>3</sup>H-CGP 12177 were 0.32 nM ( $\beta$ trunc), 0.85 nM ( $\beta$ 6-m23), 0.34 nM ( $\beta$ 36) and 0.88 nM ( $\beta$ 36-m23)<sup>40</sup>. For the competition assays, all data points on each binding curve were performed in triplicate and each 96-well plate also contained 6 determinations of total and non-specific binding. In all cases, the competing ligand completely inhibited the specific binding of <sup>3</sup>H-CGP 12177. A one-site sigmoidal response curve was then fitted to the data using Graphpad Prism 2.01 and the IC<sub>50</sub> was then determined as the concentration required to inhibit 50% of the specific binding as previously described<sup>41</sup>.

The ability of the receptors to couple to G proteins and induce an increase in cAMP concentrations was determined by measuring the increase in secreted alkaline phosphatase (SPAP) under the transcriptional control of a cAMP response element (CRE). Cells were grown to confluence in clear plastic tissue culture treated 96-well plates and CRE-SPAP secretion into the media measured between 5 and 6 hours after the addition of agonist as previously described (Supplementary Figure 1 and Supplementary Table 3)<sup>41</sup>.

## Binding of agonists to $\beta_1$ AR mutants expressed in insect cells for structural studies

Receptors  $\beta$ 36 and  $\beta$ 36-m23 were expressed using the baculovirus expression system in insect cells (High Five™) as previously described<sup>30</sup>. Cells were disrupted by freeze-thaw and membranes prepared by centrifugation. Saturation binding and competition binding experiments were performed using <sup>3</sup>H-dihydroalprenolol as previously described<sup>42</sup>. Non-specific binding of radioligand to the receptor was determined by including 100  $\mu$ M unlabelled alprenolol. The assay mixtures were incubated for 2 hours at 30°C and then filtered on a 96-well glass-fibre filter plates (Millipore) pre-treated with polyethyleneimine. The filters were washed three times with ice-cold buffer (Tris 20 mM pH 8, NaCl 150 mM), dried, and counted in a Beckmann LS 6000 scintillation counter. The apparent IC<sub>50</sub> values were determined by nonlinear regression analysis using a one-site competition model in Prism software and K<sub>i</sub> values were determined using the Cheng-Prusoff equation<sup>43</sup>.

## References

1. Evans BA, et al. Ligand-directed signalling at beta-adrenoceptors. *Br J Pharmacol.* 2010; 159:1022–1038. [PubMed: 20132209]
2. Rosenbaum DM, Rasmussen SG, Kobilka BK. The structure and function of G-protein-coupled receptors. *Nature.* 2009; 459:356–363. [PubMed: 19458711]
3. Ballesteros JA, Weinstein H. Integrated methods for the construction of three dimensional models and computational probing of structure function relations in G protein-coupled receptors. *Methods Neurosci.* 1995; 25:366–428.
4. Strader CD, et al. Conserved aspartic acid residues 79 and 113 of the beta-adrenergic receptor have different roles in receptor function. *J Biol Chem.* 1988; 263:10267–10271. [PubMed: 2899076]
5. Sato T, Kobayashi H, Nagao T, Kurose H. Ser203 as well as Ser204 and Ser207 in fifth transmembrane domain of the human beta2-adrenoceptor contributes to agonist binding and receptor activation. *Br J Pharmacol.* 1999; 128:272–274. [PubMed: 10510435]

6. Liapakis G, et al. The forgotten serine. A critical role for Ser-203<sup>5,42</sup> in ligand binding to and activation of the beta 2-adrenergic receptor. *J Biol Chem.* 2000; 275:37779–37788. [PubMed: 10964911]
7. Strader CD, et al. Identification of two serine residues involved in agonist activation of the beta-adrenergic receptor. *J Biol Chem.* 1989; 264:13572–13578. [PubMed: 2547766]
8. Wieland K, et al. Involvement of Asn-293 in stereospecific agonist recognition and in activation of the beta 2-adrenergic receptor. *Proc Natl Acad Sci U S A.* 1996; 93:9276–9281. [PubMed: 8799191]
9. Suryanarayana S, Kobilka BK. Amino acid substitutions at position 312 in the seventh hydrophobic segment of the beta 2-adrenergic receptor modify ligand-binding specificity. *Mol Pharmacol.* 1993; 44:111–114. [PubMed: 8101966]
10. Kikkawa H, Isogaya M, Nagao T, Kurose H. The role of the seventh transmembrane region in high affinity binding of a beta 2-selective agonist TA-2005. *Mol Pharmacol.* 1998; 53:128–134. [PubMed: 9443940]
11. Isogaya M, et al. Identification of a key amino acid of the beta2-adrenergic receptor for high affinity binding of salmeterol. *Mol Pharmacol.* 1998; 54:616–622. [PubMed: 9765503]
12. Cherezov V, et al. High-resolution crystal structure of an engineered human beta2-adrenergic G protein-coupled receptor. *Science.* 2007; 318:1258–1265. [PubMed: 17962520]
13. Warne T, et al. Structure of a beta1-adrenergic G-protein-coupled receptor. *Nature.* 2008; 454:486–491. [PubMed: 18594507]
14. Hanson MA, et al. A specific cholesterol binding site is established by the 2.8 Å structure of the human beta2-adrenergic receptor. *Structure.* 2008; 16:897–905. [PubMed: 18547522]
15. Wacker D, et al. Conserved binding mode of human beta2 adrenergic receptor inverse agonists and antagonist revealed by X-ray crystallography. *J Am Chem Soc.* 2010; 132:11443–11445. [PubMed: 20669948]
16. Tate CG, Schertler GF. Engineering G protein-coupled receptors to facilitate their structure determination. *Curr Opin Struct Biol.* 2009; 19:386–395. [PubMed: 19682887]
17. Kobilka BK, Deupi X. Conformational complexity of G-protein-coupled receptors. *Trends Pharmacol Sci.* 2007; 28:397–406. [PubMed: 17629961]
18. Park JH, et al. Crystal structure of the ligand-free G-protein-coupled receptor opsin. *Nature.* 2008; 454:183–187. [PubMed: 18563085]
19. Scheerer P, et al. Crystal structure of opsin in its G-protein-interacting conformation. *Nature.* 2008; 455:497–502. [PubMed: 18818650]
20. Engelhardt S, Grimmer Y, Fan GH, Lohse MJ. Constitutive activity of the human beta(1)-adrenergic receptor in beta(1)-receptor transgenic mice. *Mol Pharmacol.* 2001; 60:712–717. [PubMed: 11562432]
21. Green SA, Rathz DA, Schuster AJ, Liggett SB. The Ile164 beta(2)-adrenoceptor polymorphism alters salmeterol exosite binding and conventional agonist coupling to G(s). *Eur J Pharmacol.* 2001; 421:141–147. [PubMed: 11516429]
22. Piscione F, et al. Effects of Ile164 polymorphism of beta2-adrenergic receptor gene on coronary artery disease. *J Am Coll Cardiol.* 2008; 52:1381–1388. [PubMed: 18940527]
23. Serrano-Vega MJ, Tate CG. Transferability of thermostabilizing mutations between beta-adrenergic receptors. *Mol Membr Biol.* 2009; 26:385–396. [PubMed: 19883298]
24. Serrano-Vega MJ, Magnani F, Shibata Y, Tate CG. Conformational thermostabilization of the beta1-adrenergic receptor in a detergent-resistant form. *Proc Natl Acad Sci U S A.* 2008; 105:877–882. [PubMed: 18192400]
25. Balaraman G, Bhattacharya S, Nagarajan V. Structural Insights into Conformational Stability of Wild-Type and Mutant b1-Adrenergic Receptor. *Biophys. J.* 2010; 99:568–577. [PubMed: 20643076]
26. Altenbach C, et al. High-resolution distance mapping in rhodopsin reveals the pattern of helix movement due to activation. *Proc Natl Acad Sci U S A.* 2008; 105:7439–7444. [PubMed: 18490656]
27. Rasmussen SG, et al. Crystal structure of the human beta2 adrenergic G-protein-coupled receptor. *Nature.* 2007; 450:383–387. [PubMed: 17952055]

28. Williams RS, Bishop T. Selectivity of dobutamine for adrenergic receptor subtypes: in vitro analysis by radioligand binding. *J Clin Invest.* 1981; 67:1703–1711. [PubMed: 6263950]
29. Katritch V, et al. Analysis of full and partial agonists binding to beta2-adrenergic receptor suggests a role of transmembrane helix V in agonist-specific conformational changes. *J Mol Recognit.* 2009; 22:307–318. [PubMed: 19353579]
30. Warne T, Serrano-Vega MJ, Tate CG, Schertler GF. Development and crystallization of a minimal thermostabilised G protein-coupled receptor. *Protein Expr Purif.* 2009; 65:204–213. [PubMed: 19297694]

## References

31. Leslie AG. The integration of macromolecular diffraction data. *Acta Crystallogr D Biol Crystallogr.* 2006; 62:48–57. [PubMed: 16369093]
32. Evans P. Scaling and assessment of data quality. *Acta Crystallogr D Biol Crystallogr.* 2006; 62:72–82. [PubMed: 16369096]
33. McCoy AJ, et al. Phaser crystallographic software. *J Appl Crystallogr.* 2007; 40:658–674. [PubMed: 19461840]
34. Murshudov GN, Vagin AA, Dodson EJ. Refinement of macromolecular structures by the maximum-likelihood method. *Acta Crystallogr D Biol Crystallogr.* 1997; 53:240–255. [PubMed: 15299926]
35. Emsley P, Lohkamp B, Scott WG, Cowtan K. Features and development of Coot. *Acta Crystallogr D Biol Crystallogr.* 66:486–501. [PubMed: 20383002]
36. Schuttelkopf AW, van Aalten DM. PRODRG: a tool for high-throughput crystallography of protein-ligand complexes. *Acta Crystallogr D Biol Crystallogr.* 2004; 60:1355–1363. [PubMed: 15272157]
37. McDonald IK, Thornton JM. Satisfying hydrogen bonding potential in proteins. *J Mol Biol.* 1994; 238:777–793. [PubMed: 8182748]
38. Jones TA, Zou JY, Cowan SW, Kjeldgaard M. Improved Methods for Building Protein Models in Electron-Density Maps and the Location of Errors in These Models. *Acta Crystallogr A.* 1991; 47:110–119. [PubMed: 2025413]
39. Davis IW, et al. MolProbity: all-atom contacts and structure validation for proteins and nucleic acids. *Nucleic Acids Res.* 2007; 35:W375–383. [PubMed: 17452350]
40. Baker JG, Proudman RGW, Tate CG. An analysis of the pharmacological effects of the thermostabilising mutations and intracellular loop deletions in the turkey  $\beta$ -adrenoceptor that were essential for its crystallisation. 2010 In preparation.
41. Baker JG, Hall IP, Hill SJ. Agonist actions of “beta-blockers” provide evidence for two agonist activation sites or conformations of the human beta1-adrenoceptor. *Mol Pharmacol.* 2003; 63:1312–1321. [PubMed: 12761341]
42. Warne T, Chirside J, Schertler GF. Expression and purification of truncated, non-glycosylated turkey beta-adrenergic receptors for crystallization. *Biochim Biophys Acta.* 2003; 1610:133–140. [PubMed: 12586387]
43. Cheng Y, Prusoff WH. Relationship between the inhibition constant (K1) and the concentration of inhibitor which causes 50 per cent inhibition (I50) of an enzymatic reaction. *Biochem Pharmacol.* 1973; 22:3099–3108. [PubMed: 4202581]



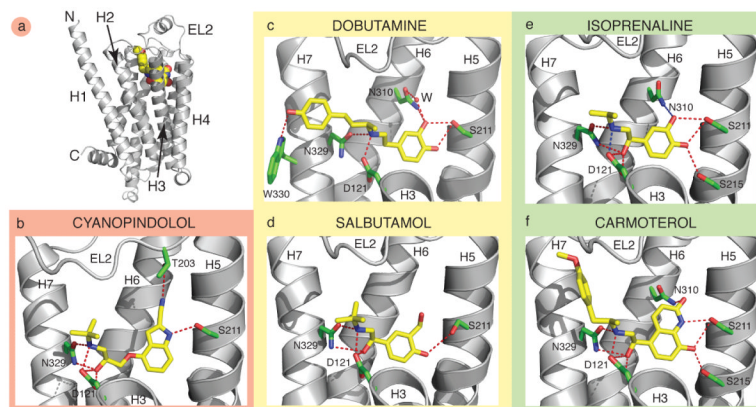


**Figure 1.** Structure of the  $\beta_1$ -adrenergic receptor bound to agonists. (a) Structure of  $\beta_1$ AR shown in cartoon representation with the intracellular side at the bottom of the figure. The ligand carmoterol is shown as a space filling model (C, yellow; O, red; N, blue). The N-terminus (N), C-terminus (C), extracellular loop 2 (EL2), and transmembrane helices 1-4 (H1-4) are labeled. The same orientation of receptor is shown in panels (b-f); (b) the antagonist cyanopindolol; (c-d) the partial agonists dobutamine and salbutamol; (e-f) the full agonists isoprenaline and carmoterol. The colour scheme of the ligand and labeling of the receptor is identical in all panes, with amino acid sidechains that make hydrogen bonds to the ligands depicted (C, green; O, red; N, blue). For clarity, residues 171-196 and 94-119 have been removed in B-F, which correspond to the C-terminal region of H4 and EL2, and EL1 with the C-terminal region of H2 and N-terminal region of H3, respectively. All structures shown are of monomer B (Supplementary Figure 2) and were generated using Pymol (DeLano Scientific Ltd). For a comparison of the positions of the ligands when bound to the receptor, see Supplementary Figure 5.

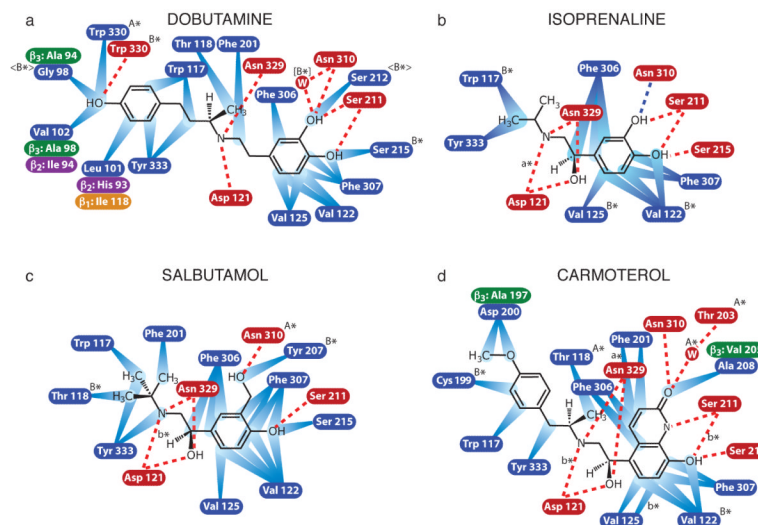


**Figure 2.**

Polar and non-polar interactions involved in agonist binding to  $\beta_1$ -adrenergic receptor. Amino acid residues within 3.9 Å of the ligands are depicted, with residues highlighted in blue making van der Waals contacts (blue rays) and residues highlighted in red making potential hydrogen bonds with favourable geometry (red dashed lines) or hydrogen bonds with unfavourable geometry (blue dashed lines). Amino acid residues labeled with an asterisk make the indicated contact either in monomer A (A\*) or in monomer B (B\*) only; for dobutamine, some contacts, labelled <B\*>, are found only in monomer B of dob92, whereas another contact, labeled [B\*], is found only in monomer B of dob102 (Supplementary Figure 6 and also see Supplementary Table 6 for further details and for the Ballesteros-Weinstein numbering). If specific van der Waals interactions or polar interactions are found only in monomer A or B, then the interaction is labeled a\* or b\*, respectively. Where the amino acid residue differs between the turkey  $\beta_1$ AR and the human  $\beta_1$ AR,  $\beta_2$ AR and  $\beta_3$ AR, the equivalent residue is shown highlighted in orange, purple or green, respectively (see also Supplementary Table 7).

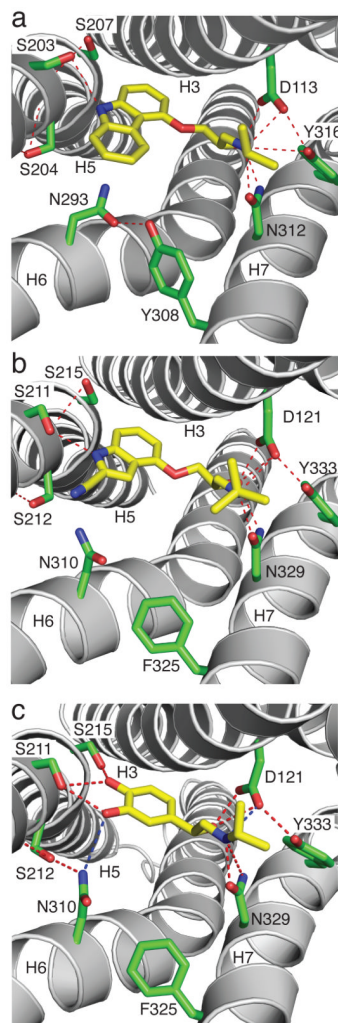


**Figure 3.** Comparison of the ligand binding pockets of the  $\beta_1$  and  $\beta_2$  adrenergic receptors. The ligand binding pockets are shown as viewed from the extracellular surface with EL2 removed for clarity (same colour scheme as in Fig. 1). (a)  $\beta_2$ AR with the antagonist carazolol bound (PDB code 2RH1); (b)  $\beta_1$ AR with the antagonist cyanopindolol bound (PDB code 2VT4); (c)  $\beta_1$ AR with the agonist isoprenaline bound.

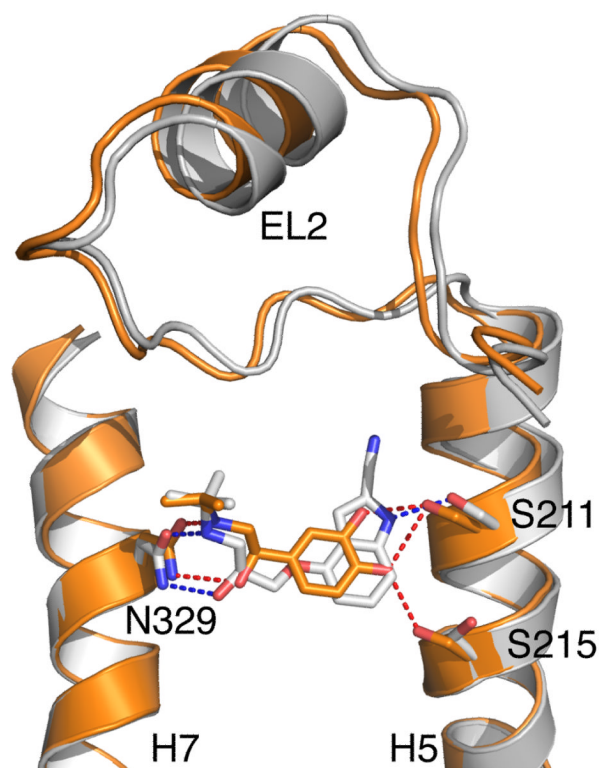


**Figure 4.** Differences in the ligand binding pocket between antagonist- and agonist-bound  $\beta_1$ -adrenergic receptor. An alignment was performed (see Online Methods) between the structures of  $\beta_1$ AR-m23 bound to either cyanopindolol (grey) or isoprenaline (orange) and the relative positions of the ligands and the transmembrane helices H5 and H7 are depicted. The 1 Å contraction of the ligand binding pocket between H5 and H7 is clear.